Prokaryotes Regulate Particulate Organic Carbon Export in Suspended and Sinking Particle Fractions

Choaro D. Dithugoe
Rhodes University https://orcid.org/0000-0003-2540-7758
Oliver K.I. Bezuidt
University of Pretoria
Emma L. Cavan
Imperial College London
William P. Froneman
Rhodes University
Sandy J. Thomalla
Council for Scientific and Industrial Research
Thulani P. Makhalanyane (thulani.makhalanyane@up.ac.za)
https://orcid.org/0000-0002-8173-1678

Research

Keywords: biological carbon pump (BCP), particulate organic matter (POM), recalcitrant dissolved organic carbon (RDOC)

Posted Date: October 20th, 2021

DOI: https://doi.org/10.21203/rs.3.rs-952425/v1

Abstract

Background

Oceans are crucial regulators of the global carbon cycle. Understanding the oceanic biological carbon pump (BCP) and its contribution to carbon export has been the subject of extensive research. These studies have provided quantitative evidence regarding the centrality of phytoplankton throughout the water column. In the Southern Ocean, the biological carbon pump is driven primarily by phytoplankton productivity and is an effective organic matter sink. There is evidence showing that sinking particulate organic matter (POM) sustains microbial communities with different ecological strategies (i.e., *r*-/*K*-strategists). These results suggest that the role of microbial communities on the effectiveness of the biological carbon pump should not be underestimated. However, we lack mechanistic insights regarding the importance of these microorganisms, their diversity and influence on the efficiency of the BCP.

Results

Here, we provide the first insights regarding prokaryotic metabolic capacity linked to suspended and sinking particles to improve our understanding of microbial contributions towards POM export in the Southern Ocean. A Marine Snow Catcher (MSC) was deployed at several stations southwest of Tasmania in the Subantarctic zone to obtain suspended and sinking particulate material for determining carbon and nitrogen flux. Metagenomic analysis and metagenomic-assembled genomes showed that both the suspended and sinking particle-pools were dominated by bacteria with metabolic capacity for degrading POM (e.g. *Gammaproteobacteria* MAGs). Archaeal genomes (*Poseidoniia* and *Nitrososphaeria*) appear to drive nitrogen metabolism via nitrite and ammonia oxidation in these communities. Results suggest that for bacteria *r*-strategists were more ubiquitous in the suspended pool while *K*-strategists were more prevalent in the sinking particle-pool, with the opposite being true for archaea. In addition, metabolic reconstructions suggest that prokaryotes harbour substantial genetic capacity for degrading complex POM and chemoautotrophic synthesis of recalcitrant dissolved organic carbon (RDOC) from CO_2.

Conclusion

The metagenome assembled genomes from sinking and suspended size fractions and carbon flux determinations revealed striking trends regarding prokaryotic contributions in the water column. The results show that the predicted lifestyles for bacteria and archaea may differ substantially in sinking and suspended fractions, suggesting niche specificity. Together, our data suggest that prokaryotes in suspended and sinking particles may enhance POM export via the production of RDOC in the Southern Ocean.

Background

The Southern Ocean plays a significant role in carbon cycling, buffering the impacts of climate change by accounting for 50% of the total oceanic uptake of CO_2 [1, 2]. Phytoplankton primary production and

carbon export to the deep ocean, i.e. the biological carbon pump (BCP) [3, 4] is considered a major contributor to the sink of natural CO_2 removing ~33% of the global organic carbon flux [5]. However, only a small fraction of the organic carbon fixed by phytoplankton in surface waters ultimately reaches the ocean interior [6, 7] and it is uncertain what factors control the fraction of production that is exported or how effectively this material is transferred to depth [8]. Factors that regulate phytoplankton growth, particle formation, rates of sinking and remineralisation all modify the extent to which fixed particulate organic carbon (POC) is transformed to dissolved organic carbon (DOC) and effectively exported and hence the efficiency of the BCP [9, 10].

Marine microbes in particular that associate with both sinking and suspended particles have been shown to mediate key processes linked to the BCP [8, 11, 12]. Microbial diversity influences the composition of DOC, which includes a diverse range of molecules that can be biologically labile (e.g. amino acids and glucose) that are rapidly remineralised by microbes in the surface ocean to produce dissolved inorganic carbon (DIC) thus reducing export efficiencies (the microbial loop) [11, 13]. Alternatively, recalcitrant DOC (RDOC) (e.g. lignin and lipids) is exported to the deep ocean, and therefore longer-term storage becomes possible [14, 15]. A small percentage of microbial DOC production is refractory (rDOC) (e.g. ~5-7% derived from glucose), which resists rapid remineralization and further degradation [16–18]. The rDOM produced by microbial degradation of complex organic carbon accumulates in the ocean interior accounting for >95% of the large DOC pool [19, 20] and this long-lived reservoir plays an important role in shaping global climate by sequestering CO from the atmosphere [21]. The RDOC and rDOC microbial production form part of the microbial carbon pump (MCP) which enhances export efficiencies by aiding the transfer of DOC to the deep ocean [22–24]. Indeed, in instances where the microbial loop dominates (i.e. a system with small-celled non-sinking particles and low POC flux) the MCP is considered the prevailing mechanism for carbon sequestration [25]. Despite the intricate role of prokaryote diversity and activity on regulating both the BCP and MCP, we lack a mechanistic understanding regarding the phylogeny and function of prokaryotes linked with suspended and sinking particle pools in the ocean.

The composition of the suspended and sinking particle pool (either labile, semi-labile, semi-recalcitrant and recalcitrant) [26] may also determine the ecological growth strategies of prokaryotes (*r*- or *K*-strategist) [27, 28]. Prokaryotes which grow rapidly or change in response to labile and semi-labile POM are regarded as *r*-strategists [29] whereas prokaryotes which slowly degrade complex high molecular weight organic compounds such as RDOC are regarded as *K*-strategists [30]. As such, a niche differentiation is expected in prokaryotic distribution based on their ability to degrade particulate organic matter (POM) [31] with r-strategists being prevalent in the sinking particle-pool where they degrade transient POC, while K-strategists are more likely to exploit the suspended particle-pool [29].

Here, we present the first assessment of prokaryotic functional capacity in sinking and suspended marine particle fractions collected with a marine snow catcher (MSC) at five stations from the Southern Ocean Time Series (SOTS) site in the sub-Antarctic zone (SAZ) during austral autumn. In addition to determining carbon and nitrogen flux, we specifically elucidate carbon and nitrogen cycling metabolic pathways linked to prokaryotes with different lifestyles (*r*- and *K*-strategists) in the suspended and sinking particle

fractions. By using metagenome-assembled genomes (MAGs) to link bacterial and archaeal genomes to POM sequestration we provide insights into the role of *r*-/*K*-strategists towards organic carbon export in the Southern Ocean.

Results

Ancillary station data

Temperature and salinity (TS) plots for all 5 stations (Supplementary Figure S1) showed very similar water mass characteristics in the surface 120 m, above the MSC sampling depth (Figure 1A). Stations 2 and 3 demonstrated slight deviations with increased salinity levels relative to temperature, but only at depths greater than 120 m. As such, any observed variability between the 5 MSC samples was unlikely the result of lateral advection but more likely a reflection of temporal adjustments in the system over the two-week sampling period. MLD's for all stations were similar and ranged from 100 - 110 m (Supplementary Table S1). Chlorophyll profiles, at stations 1 to 3, exhibited a subsurface maximum at ~30 m indicative of surface nutrient limitation. Stations 4 and 5 were homogenous throughout the mixed layer (Supplementary Figure S2a). MLD integrated chlorophyll was highest at stations 1 and 2 (106 and 104 mg m^{-3} respectively) and lowest at station 4 (86 mg m^{-3}) (Supplementary Figure S2b).

Variations in POC and PON in the suspended and sinking particle-pools

Despite relatively similar water mass and chlorophyll biomass characteristics between stations, the differences in POC and PON flux and distribution between stations were substantial. The large majority of POC was observed in the suspended particle pool (84% ±11%) with only a small percentage found in the sinking pool (16% ±11%) (Figure 1B). PON levels demonstrated the opposite trend with the highest values observed in the sinking pool (68% ±14%) compared to the suspended pool (32% ±14%) (Figure 1C). The distribution of PON between stations was also different, with the highest levels (in both the suspended and sinking fractions) occurring at station 3 (87 and 29 µg l^{-1}, respectively) compared to all other stations (< 20 µg l^{-1}) (Figure 1D), which drove the highest PON flux at station 3 (31 mg m^{-2} d^{-1}) (Figure 1E). For POC, the highest concentrations for sinking pools were found at station 2 (96 µg l^{-1}), which consequently had the highest POC flux (34 mg m^{-2} d^{-1}); an order of magnitude higher than the POC flux observed at station 4 (3 mg m^{-2} d^{-1}). In contrast, suspended POC was highest at stations 2 and 3 (222 and 252 µg l^{-1}, respectively). This variability drove large differences in suspended and sinking POC:PON ratios, which were particularly high in the suspended fraction, at stations 1 and 2 (31 and 40 POC:PON, respectively) compared to all other stations (<9) (Figure 2c). In the sinking fraction, the highest ratios were similarly found at stations 1 and 2 (2 and 6 POC:PON, respectively) compared to all other stations (<1).

Taxonomic profiles and MAG reconstruction

The core shared operational taxonomic units (OTUs) by suspended and sinking particle fractions with 80% frequency cut off in both bacterial and archaeal communities. Bacterial communities shared 81.8% OTUs while ~1.1% (suspended) and ~1.9% (sinking) were unique (Figure 2A). Similarly, the archaeal community shared 89.1% OTUs while ~4.2% (suspended) and ~1.2% (sinking) were unique. Classification at class level revealed that bacterial communities were dominated by *Alphaproteobacteria*, *Gammaproteobacteria* and *Bacteroidia* in all stations for both the sinking and suspended fractions (Figure 2C). Differences between stations were evident in the remaining, less dominant taxa, with *Magnetococcia and Verrucomicrobia* occurring at Stations 1 and 2, while *Oxyphotobacteria* were present at Stations 3 to 5 (Supplementary Figure S3a). Very little difference was observed in bacterial community distribution when comparing the suspended and sinking particle-pools across all stations. Inter-station differences were more apparent in the distribution of archaeal lineages (Supplementary Figure S3b). The suspended particle-pool was dominated by *Methanosarcinia*, *Thermoplasmata* and *Archaeoglobi* while the sinking particle-pool was dominated by *Thermoplasmata*, *Thermoprotei* and *Methanomicrobia* (Figure 2). Stations 1 and 2 were dominated by *Nitrosophaeria*, *Thermoplasmata* and *Methanomicrobia* (Figure 2D). Stations 4 and 5 were also dominated by members of *Nitrosophaeria*, *Thermoplasmata* and *Methanosarcinia*. Similar to bacterial communities, very little difference was observed when comparing archaea in the suspended and sinking particle-pools. Archaeal community composition at station 3 was the most diverse and displayed the largest difference between suspended and sinking fractions.

In total, 24 medium quality MAGs were recovered (11 from the suspended and 13 from the sinking particle-pool fractions) (Supplementary Table S2). Taxonomic classification revealed that 5 MAGs were affiliated with *Gammaproteobacteria*, with 4 recovered from the sinking particle pool (stations 3 - 5) and only one from the suspended fraction (station 2). In total, 6 MAGs were affiliated with *Cyanobacteriia*, and these were split evenly between the sinking and suspended particle pools from stations 3 to 5. The remaining MAGs were classified as *Poseidoniia* (9 in total occurring in both the suspended and sinking fractions at all stations except station 3) and *Nitrososphaeria* (4 in total occurring in both the suspended and sinking fractions at stations 1 and 2). The ANI scores of all bacterial and archaeal MAGs were below 90%, against 1254 bacterial (*Cyanobacteriia* and *Gammaproteobacteria*) (Figure 3A) and 4 957 archaeal (*Thermoplasmatota* and *Thaumarchaeota*) (Figure 3B) RefSeq complete genomes, respectively.

Read recruitment and functional profiling of MAGs from the suspended and sinking particle-pools

Raw reads were mapped against reconstructed MAGs using CoverM. For all the 24 MAGs, functional profiles linked to central, nitrogen and carbon metabolism were predicted based on the DRAM pipeline. Read recruitment, against all bacterial MAGs, suggests that *Gammaproteobacteria* were relatively more abundant in the suspended than the sinking fraction at station 1, 4 (suspended) and station 5 (sinking) (Supplementary Figure S3A). Specifically, SK1_Gammaprotebacteria and SK5_Gammaprotebacteria_b MAGs were relatively abundant at station 1 (suspended), 2 (sinking and suspended) and 5 (sinking). Whereas SP2_Gammaprotebacteria and SK5_Gammaprotebacteria_a are relatively abundant in the

sinking particle-pool fractions. *Cyanobacterial* MAGs were relatively abundant at station 3 and present at station 1, 2, 4 and 5. Bacterial MAGs potential function revealed that they are methanotrophs and that they harbour CAZymes involved in degradation of chitin with the exception of SK5_Gammaproteobacteria_b (Figure 4A). All bacterial MAGs harboured the capacity to convert acetate to methane with the exception of SK1_Gammaproteobacteria, which harboured a pathway for converting trimethylamine to dimethylamine. Additionally, *Gammaproteobacterial* MAGs harboured a suite of CAZymes involved in complex POM degradation, most notably linked to the sinking fraction of samples recovered at station 2 and 5. *Gammaproteobacterial* MAGs also harboured genes linked to short chain fatty acid (SCFA) and alcohol conversions for degradation of labile and complex POM. The SK2_Gammaprotebacteria MAG in particular possessed most CAZymes and was the only MAG involved in nitrogen metabolism, through the use of nitrite oxidoreductases which converts nitrite to nitrite oxide. Bacterial MAGs harboured multiple central and energy metabolic pathways including glycolysis, Krebs cycle, pentose phosphate pathway, glyoxylate cycle, Calvin cycle, Arnon-Buchanan cycle, dicarboxylate-hydroxybutyrate cycle, Wood-Ljungdahl pathway and hydroxypropionate bi-cycle (Supplementary Figure S4A). Only *Cyanobacteriia* and SK2_Gammaproteobacteria possessed genes related to the Entner-Doudoroff pathways, which converts phosphorylated glucose molecules to use as carbon and energy sources.

Poseidoniia and *Nitrososphaeria* archaeal MAGs are relatively abundant across all samples with the exception of station 3 (absent in both sinking and suspended) (Supplementary Figure S3B). These archaeal MAGs are more relatively abundant in the suspended than the sinking particle-pools at stations 1 and 2 and evenly abundant at station 3. *Nitrososphaeria* MAGs were methanogens/methanotrophs, which were reconstructed at station 1 (sinking and suspended) and station 2 (sinking). These *Nitrososphaeria MAGs* are involved in nitrogen metabolism via nitrite oxidoreductase and ammonia oxidation, and they are involved in the conversion of short chain fatty acids (SCFA) and alcohol (Figure 4B). Interestingly, a *Nitrososphaeria* MAG from the sinking fraction of station 2 possessed CAZy genes involved in the degradation of polyphenolics and involved in the SCFA and alcohol conversion pathway. Archaeal MAGs from *Poseidoniia* on the other hand are all implicated in the conversion of SCFA and alcohol. *Poseidoniia* MAG on the suspended fraction at station 1 were classified as a methanogen/methanotrophs and contained the nitrite oxidoreductase (Figure 4B). *Nitrososphaeria* and *Poseidoniia* MAGs harboured a similar central and energy metabolism as bacteria lacking the Entner-Doudoroff pathway. Functional reconstruction suggests that *Nitrososphaeria* MAGs lack the Wood-Ljungdahl pathway (Supplementary Figure 4B). Archaeal MAGs possess methanogenesis pathways, with evidence that they may be able to convert CO_2 to methane, as part of their central metabolism.

Discussion

POC and PON are considered the main resource supporting diverse microbial communities in both the suspended and sinking particle-pools [27]. The range of activities associated with this diverse community of microbes alters the nature of the particulate and dissolved pool and thus contributes to the quantity of

carbon or nitrogen, which is effectively exported below the seasonal mixed layer. As such, an understanding of the prokaryotic community composition and their functional capacity on both sinking and suspended particles may facilitate a more mechanistic understanding of microbial contributions to POC/PON degradation and/or synthesis. This study expands our understanding of the prokaryotic community contributions to organic carbon and nitrogen export by providing the first metagenome assembled genomes from suspended and sinking particle pool fractions in the Southern Ocean.

Differences in prokaryotes may explain the divergence in POC and PON concentration in both the sinking and suspended particle pools

Recent studies have shown a positive relationship between phytoplankton biomass and the magnitude of POM export [32, 33]. These findings were corroborated by our data showing a positive relationship between MLD integrated chlorophyll and POM flux. However, this relationship was poor (r^2 = 0.33 for POC and r^2 = 0.06 for PON) suggesting that phytoplankton biomass may only account for ~30% of carbon flux variability and as little as ~6% of nitrogen flux variability. This is perhaps unsurprising considering the many factors that influence the concentration of POM, which is effectively exported out of the surface layer (e.g. sinking rates and prokaryotic activity etc.) [34, 35]. Previous studies have demonstrated that POM content (labile, semi-labile, recalcitrant, or refractory), rather than POM concentration, is the main driver of prokaryotic community structure [36, 37]. There is also evidence showing that as POM sinks through the mesopelagic zone it is subjected to degradation by several free-living and particle-associated prokaryotes [29]. As such, prokaryotes alter the chemical constituency of POM and may in turn also contribute as secondary drivers of change, altering their community structure [22, 38]. Labile or semi-labile [39], recalcitrant or refractory DOM production [40] from prokaryotic degradation of POM includes the production of so called ‘sticky polysaccharides’, which form part of the aggregation of DOM into suspended POM and sinking POM [41]. In this instance, both the suspended and sinking POM serve as the main source of carbon and energy for prokaryotes in the mesopelagic [42, 43]. Since POC flux to the mesopelagic is insufficient to support the carbon demand of prokaryotes, suspended particles are considered a major sustaining source of organic carbon for microbes in the mesopelagic [29]. While the concentration of POC in sinking particles decreases exponentially with depth, the concomitant POC concentration in suspended particles remains largely constant and is typically ~1-2 orders of magnitude higher than that of sinking particles [29]. This finding is similar to our POC data, which was substantially higher in the suspended vs sinking fraction. However, the same was not true for PON with more PON concentration at stations 1-3 and similar PON concentration at stations 4 and 5 in the sinking material when compared to suspended.

Several factors may account for the widespread variability in the POC:PON ratio observed on suspended and sinking samples in this study. These include i) the preferential degradation of nitrogen rich POM [44] (most notably in the suspended samples at stations 1 and 2 where POC:PON ratios were >30), ii) the synthesis of refractory POC resistant to further degradation [45], which would also drive high POC:PON ratios, iii) chemoautotrophic microbial activity on the POM, increasing the POC:PON ratio [46] and iv) the oxidation of sinking POC by marine microbiota [47], which may drive a preferential reduction in POC

relative to PON, thereby decreasing POC:PON ratios as evidenced in all sinking samples where POC:PON ratios were less than the Redfield ratio of 6.6. Despite the large differences in the distribution of POC:PON ratios between suspended and sinking samples, and between stations, the bacterial community composition was very similar. This suggests that variability in POC:PON ratios may be a product of variability of microbial activity despite similarities in bacterial community structure. On the other hand, differences were observed in archaeal communities such that the PON content might have been different between stations. Alternatively, the composition of the source material may have been similar but may be acted upon differently by the bacteria and archaea driving secondary changes in their community structure [12, 22, 48]. Evidence for this argument can be seen in the relative abundance of bacterial MAGs, which demonstrates variability in prokaryotic activity between suspended and sinking pools, and between stations, despite similarities in community composition. As such, our results suggest that differences in prokaryotic activity rather than diversity, particularly in the case of bacteria, impact the signature of POC and PON in both sinking and suspended material. Nevertheless, examples of the impact of archaeal diversity on POC:PON variability (although most likely secondary) are evident when observing *Nitrososphaeria*, which were highest at stations 1 and 2 where the highest POC:PON ratios were encountered, together with the highest POC flux (most notably at station 2). This implies that *Nitrososphaeria* may be actively involved in PON degradation, a notion that is corroborated by the presence of nitrogen metabolism in *Nitrososphaeria* at stations 1 and 2. Conversely, station 3 had the least amount of *Nitrososphaeria* and observed a particularly high PON flux relative to all other stations.

Prokaryotic ecological strategists based on POC and PON content

Prokaryotes may exhibit different ecological strategies in response to POC content [49, 50]. Previous studies suggest that *r*-strategists may be more prevalent in sinking particle-pools where they degrade transient POM [50, 51], whereas *K*-strategists appear to exploit complex compounds (e.g. RDOM) from the suspended particle-pool [29, 50]. As such, a niche differentiation would be expected in prokaryotic community and functional activity between sinking and suspended pools. However, prokaryotes are also known to detach from sinking particles, potentially enhancing the suspended particle-pool with microbiota that are similar to the sinking particle-pool [27]. Metabolic activities associated with *K*-strategists include CO_2 fixation via the Wood-Ljungdahl pathway, the Calvin cycle, Arnon-Buchanan cycle and the Hydroxypropionate-hydroxybutyrate cycle by condensing two molecules of CO_2 as electron acceptor and hydrogen as electron donor into Acetyl-CoA as building blocks for biosynthesis. Prokaryotes exhibiting these metabolic activities are typically chemoautotrophs, which synthesise complex organic carbon such as RDOM or polysaccharides polymers from CO_2 [52].

In our results, these chemoautotrophic bacteria MAGs, typical of *K*-strategists, were more prevalent in the sinking particle pool than the suspended pool, which is in contrast to previous studies [29]. However, it is likely that any metabolic activity which uses POM to form polymers may consequently initiate aggregation and subsequent sinks enhancing POM export flux, thus accounting for their presence on

sinking material. On the other hand, there was no discernible difference in the functional profiles between suspended and sinking material associated with *r*-strategists and *K*-strategist, respectively. For example, bacterial MAGs from *Gammaproteobacteria* were present in both the sinking and suspended sample at station 2 and possessed CAZymes involved in the degradation of labile POM such as diatom-derived POM [53], grass POM [54], and virus-induced POC from picocyanobacterial and polysaccharides [55], whose expected role would be to reduce carbon flux via particle degradation while sinking into the mesopelagic. Similarly, all bacterial MAGs were associated with the degradation of chitin, regardless of their association with sinking or suspended material. Chitin is rich in both carbon and nitrogen and can be reintegrated into biomass forming polysaccharide polymers or mineralized to enrich the water column with inorganic carbon and nitrogen, reducing both the POC and PON export flux [56]. As such, our results suggest that a combination of microbial driven transition between suspended particles and the formation of aggregates (e.g. via the synthesis of sticky polysaccharides) and the dissociation of microbes from the sinking particle pool to the suspended particle pool [27] make it difficult to discern any specific bacterial preference of *r*-/*K*-strategists for one particle type over another. This is contrary to some studies which suggest specific biogeochemical roles for prokaryotes in suspended and sinking particle-pools in the marine carbon cycle [29].

On the other hand, our chemoautotrophic archaea MAGs mostly *Nitrososphaeria* were determined to be more prevalent at station 1 and 2 (suspended only) and relatively less abundant at stations 3 to 5 (both suspended and sinking fractions). As with bacteria, chemoautotrophic archaeal MAGs appear to be *K*-strategists and are expected to dominate the suspended particle pool, which was indeed the case for our samples at stations 1 and 2. This is more in-line with predicted archaeal MAGs distribution that is said to be more dominant in *r*-strategists where they scavenge for PON in the suspended particle-pool [57]. The ammonia oxidizing archaea (AOA) present on sinking samples at stations 1 and 2 (*Nitrososphaeria*) and the suspended sample at station 1 (*Poseidoniia*) directly utilise simple and complex organic nitrogen as their main source of ammonia and nitrite [58]. Based on the POC:PON ratio it appears that the suspended particle-pool might be more influenced by AOA resulting in low concentrations of PON relative to POC in the suspended fraction, driving ratios in the suspended material that far exceed Redfield at all stations reaching >30 at stations 1 and 2. Surprisingly, *Cyanobacteriia* had no genes linked to the nitrogen metabolism pathway. However, the sinking sample at station 2 possessed genes for nitrogen metabolism and also had the highest POC:PON ratio. Nitrogen metabolism was also more prevalent in archaeal compared to bacterial MAGs. The presence of AOA (*Nitrososphaeria* and *Poseidoniia*), NOB (*Gammaproteobacteria*) and NOA (*Nitrososphaeria*) MAGs at station 1 (suspended and sinking) and station 2 (suspended) had the highest POC:PON ratio, the highest POC flux and the lowest PON flux. These NOB/NOA and AOA are obligatory partners where the NOB/NOA catalyse the degradation of PON to ammonia for the nitrite producing AOA partner [59]. This may explain the decrease in PON export flux observed at station 1 and 2. NOB/NOA, and AOA are also key players in the removal of nitrogen from PON, increasing the POC:PON ratio at station 1 and 2, thereby increasing the POC export flux relative to PON export flux. In addition to preferential degradation of PON, Archaeal MAGs may also be involved in

the synthesis of RDOC, enriching the water column with organic carbon particles, increasing POC export flux relative to the PON flux [60].

Although *Cyanobacteriia* are well known photosynthetic microbes involved in nitrogen fixation, the fact that our MAGs showed no evidence for nitrogen fixation is surprising [61, 62]. A possible reason for this may be the presence of non-cyanobacterial diazotrophs (NCD), such as dinitrogen (N_2) fixing bacteria and archaea [63]. Indeed, *Gammaproteobacteria* (on the sinking sample at station 2) were the only bacterial MAG containing nitrogen metabolism, while *Nitrososphaeria* were also present at station 1 and 2. *Poseidoniia* MAG at station 1 (suspended) also had metabolic capacity for nitrogen metabolism. Coincidentally, these were the two stations with the highest POC:PON ratio (and highest carbon flux) indicative of preferential nitrogen uptake by the prokaryotic community. Since phytoplankton biomass can account for only ~6% of the nitrogen flux, the high PON flux observed in station 3 to 5 might be due to prokaryotic activity on PON by assimilating the available inorganic nitrogen into its biomass [64]. The dissimilation of inorganic nitrogen from PON [65] which favours PON export is thus more likely to be a result of prokaryotic activity than phytoplankton biomass.

Conclusion

Our results suggest that differences in prokaryotic activity, rather than diversity particularly in the case of bacteria, impact the signature of POC and PON in both the sinking and suspended material. However, PON content may act as a secondary driver of change in archaeal community structure following the alteration of the chemical constituency of POM. The variability in the archaeal communities and functional traits may impact the POM flux. This is particularly true for nitrogen metabolism from PON by *Nitrososphaeria*, which regulates high POC flux when present as opposed to high PON flux in the absence of nitrogen metabolism. Contrary to previous studies, our data suggest that prokaryotic activity on suspended particles, their metabolic capacity to form aggregates (e.g. via the synthesis of sticky polysaccharides) and their dissociation from sinking to suspended particle-pools may confound the ecological niche of these microbes. On the other hand, our archaeal MAGs were consistent with the predicted dominance of *r*-strategists scavenging PON in the suspended particle-pool. The connection between AOA and NOB/NOA may contribute to the dissimilatory nitrogen metabolism from PON, thus, reducing PON flux relative to POC flux in the Southern Ocean. The relationship between phytoplankton as primary regulators of POM content and prokaryotes acting on POM as a secondary driver of change in POM levels complicate efforts to disentangle the precise biogeochemical function in the suspended and sinking particle-pools. However, mechanistic laboratory studies may provide insights regarding phytoplankton and prokaryotes trophic interactions and their ultimate contribution to POM export flux in the ocean.

Material And Methods

Site description and cruise details

The SOTS is Australia's contribution to the international Ocean SITES global network of time series observatories (http://www.oceansites.org/). The site is located at 47°S and 142°E, approximately 530 km southwest of Tasmania in the Indian/Australian sector of the SAZ [66]. Samples were collected from five MSC stations (Figure 1A) over the course of 2 weeks between March and April 2019 aboard the RV Investigator. At each station, CTD deployments provided temperature, salinity, and fluorescence derived chlorophyll profiles. The mixed layer depth (MLD) was calculated from temperature profiles with a threshold criterion of 0.2ºC as detailed previously [67].

MSC Sample collection

The MSC was deployed at five stations (Supplementary Table 1) at 10 m below the MLD following the method described by Riley, Sanders, Marsay, Le Moigne, Achterberg and Poulton [68] (see Supplementary methods). A MSC acts as a settling chamber allowing the separation of suspended (top of the MSC) and sinking (bottom of the MSC) samples after 2 hours of settling. After sampling, both the suspended and sinking particle-pools were homogenised and divided using a Folsom splitter for POC, particulate organic nitrogen (PON) and molecular analysis. Sub-samples for POC/PON analysis were filtered onto pre-combusted (450°C, 12 h) glass fibre filters (47 mm diameter GF/F, Whatman) using a vacuum filtration pump at a pressure of -0.2 bar. The resultant filters were placed in sterile petri-dishes and oven dried overnight at 25°C. This was followed by acid fumigation with concentrated hydrochloric acid overnight to remove inorganic carbon. Filters were then punched and folded into aluminium tin cup foils. The samples were analysed in the Department of Archaeology at the University of Cape Town on a Flash 2000 organic elemental analyser (Thermo Fisher Scientific, Waltham, MA, USA). The POC/PON concentrations for the sinking fraction were adjusted based on the assumption that suspended POC/PON was homogenous throughout the MSC before settling (ie. the concentration of the suspended fraction was subtracted from the sinking fraction) [68]. The POC and PON flux was calculated by dividing the sinking mass (mg) with the MSC area (0.06 m^{-2}). The resulting value was then divided by the settling time (days) and multiplied by the ratio of the sampled sinking volume (0.87) modified based on the MSC design [69].

Molecular analysis and sequencing

To explore the composition and function of microorganisms associated with the suspended and sinking particle-pools, 2 litres of water from both fractions was filtered using 0,2 µm pore-size polycarbonate membrane filters (47 mm diameter, Millipore (Burlington, Massachusetts, United States) as detailed previously [70]. The filters were stored at -80°C until further processing. DNA was extracted using the Power Soil kit (QIAGEN, Hilden, Germany) as described by Hirai, Nishi, Tsuda, Sunamura, Takaki and Nunoura [71]. The resultant DNA was assessed using Qubit 4 Fluorometer (Thermo Fisher Scientific, Waltham, MA, USA). High quality DNA was sequenced by Admera Health Biopharma Services (South Plainfield, USA). Library preparation was performed using the Nextera XT DNA Library Preparation Kit (Illumina, California, USA) as recommended by the manufacturer. The library was quantified using the KAPA SYBR® FAST qPCR with Quant Studio ® 5 System (Applied Biosystems). The libraries were pooled

(equimolar concentrations) and sequenced using an Illumina® HiSeq (Illumina, California, USA) using the 2x150 paired end chemistry.

Taxonomic classification and MAG reconstruction

The quality of raw metagenomic data was assessed using FastQC (https://github.com/s-andrews/FastQC). The reads were processed to remove sequencing adapters and low-quality reads using Trimmomatic v.0.36 [72]. These reads were used for taxonomic classification, using the default parameters in SingleM v0.13.2 (https://github.com/wwood/singlem). The ATLAS workflow [73] was used to assemble raw reads and for generating MAGs using the default parameter settings. CheckM v1.1.3 was used to assess the quality of MAGs as detailed previously [74]. Following genome reporting standards, MAGs with genome completeness scores >50% and <10% contamination were selected for downstream analysis [75]. The Genome Taxonomy Database toolkit (GTDB-Tk) v1.5.0 [76] was used to assign taxonomy to all MAGs. Phylogenetic diversity of the reconstructed MAGs was inferred against complete archaeal and bacterial genomes acquired from the NCBI RefSeq database using the FastANI v1.32 tool [77]. To estimate the relative abundance of each taxa, MAGs from the suspended and sinking particle-pools were mapped using default parameters in CoverM v0.6.1 (https://github.com/wwood/CoverM). Functional profiles for all MAGs were obtained by using DRAM v1.2.0 [78].

Declarations

Availability of data and information

Southern Ocean Time Series, 10 raw metagenomic sequence reads are available at the NCBI (https://dataview.ncbi.nlm.nih.gov/object/PRJNA749920?reviewer=sci0fvulcn2e27bu98nb1m2d4g).

Acknowledgments

We wish to thank Australia’s Integrated Marine Observing System (IMOS), which is enabled by the National Collaborative Research Infrastructure Strategy (NCRIS). It is operated by a consortium of institutions as an unincorporated joint venture, with the University of Tasmania as Lead Agent. The MSC sampling at SOTS was made possible by to Philip Boyd (Institute for Marine and Antarctic Studies, University of Tasmania), Thomas Trull (CSIRO, Tasmania, Australia) and Mathew Bressac (Institute for Marine and Antarctic Studies, University of Tasmania) using the RV Investigator IN2019_V02 (GIpr08) research ship. This work was supported through the CSIR’s Southern Ocean and Carbon Climate Observatory (SOCCO) Programme (http://socco.org.za/) funded by the Department of Science and Innovation (DST/CON 0182/2017) and the CSIR’s Parliamentary Grant. In addition, we acknowledge funding from the National Research Foundation (NRF) Grant No: 110729. We acknowledge Laique Djeutchouang, Natasha Van Horsten and Thomas Ryan-Keogh for assistance with python scripts.

Author contributions

S.J.T and TPM conceived the study, supervised the research and funded the analysis. C.D.D performed the experiments, analysed the data, contributed to experimental design, and wrote the manuscript. O.KI.B assisted with the bioinformatic analysis. E.L.C., W.P.F. and S.J.T contributed to the analysis of oceanographic data. All authors edited, read and approved the final version of the manuscript.

Competing interests

All authors declare that they have no competing interests.

References

1. DeVries T, Holzer M, Primeau F. Recent increase in oceanic carbon uptake driven by weaker upper-ocean overturning. Nature. 2017;542:215–8. doi:10.1038/nature21068.
2. Friedlingstein P, Jones MW, O'Sullivan M, Andrew RM, Hauck J, Peters GP, Peters W, Pongratz J, Sitch S, Le Quere C, Bakker DCE, Canadell JG, Ciais P, Jackson RB, Anthoni P, Barbero L, Bastos A, Bastrikov V, Becker M, Bopp L, Buitenhuis E, Chandra N, Chevallier F, Chini LP, Currie KI, Feely RA, Gehlen M, Gilfillan D, Gkritzalis T, Goll DS, Gruber N, Gutekunst S, Harris I, Haverd V, Houghton RA, Hurtt G, Ilyina T, Jain AK, Joetzjer E, Kaplan JO, Kato E, Goldewijk KK, Korsbakken JI, Landschutzer P, Lauvset SK, Lefevre N, Lenton A, Lienert S, Lombardozzi D, Marland G, McGuire PC, Melton JR, Metzl N, Munro DR, Nabel JEMS, Nakaoka SI, Neill C, Omar AM, Ono T, Peregon A, Pierrot D, Poulter B, Rehder G, Resplandy L, Robertson E, Rodenbeck C, Seferian R, Schwinger J, Smith N, Tans PP, Tian HQ, Tilbrook B, Tubiello FN, van der Werf GR, Wiltshire AJ, Zaehle S. Global Carbon Budget 2019. Earth System Science Data. 2019;11:1783–838. doi:10.5194/essd-11-1783-2019.
3. Boyd PW, Claustre H, Levy M, Siegel DA, Weber T. Multi-faceted particle pumps drive carbon sequestration in the ocean. Nature. 2019;568:327–35. doi:10.1038/s41586-019-1098-2.
4. Henson S, Le Moigne F, Giering S. Drivers of Carbon Export Efficiency in the Global Ocean. Global Biogeochem Cycles. 2019;33:891–903. doi:10.1029/2018GB006158.
5. Schlitzer R. Carbon export fluxes in the Southern Ocean: results from inverse modeling and comparison with satellite-based estimates. Deep Sea Res Part II. 2002;49:1623–44. doi:10.1016/s0967-0645(02)00004-8.
6. Martin JH, Knauer GA, Karl DM, Broenkow WW. VERTEX: carbon cycling in the northeast Pacific. Deep Sea Research Part A Oceanographic Research Papers. 1987;34:267–85. doi:10.1016/0198-0149(87)90086-0.
7. Giering SL, Sanders R, Lampitt RS, Anderson TR, Tamburini C, Boutrif M, Zubkov MV, Marsay CM, Henson SA, Saw K, Cook K, Mayor DJ. Reconciliation of the carbon budget in the ocean's twilight zone. Nature. 2014;507:480–3. doi:10.1038/nature13123.
8. Cavan EL, Le Moigne FAC, Poulton AJ, Tarling GA, Ward P, Daniels CJ, Fragoso GM, Sanders RJ. Attenuation of particulate organic carbon flux in the Scotia Sea, Southern Ocean, is controlled by zooplankton fecal pellets. Geophys Res Lett. 2015;42:821–30. doi:10.1002/2014gl062744.

9. De La Rocha CL, Passow U. Factors influencing the sinking of POC and the efficiency of the biological carbon pump. Deep Sea Res Part II. 2007;54:639–58. doi:10.1016/j.dsr2.2007.01.004.
10. Talmy D, Martiny AC, Hill C, Hickman AE, Follows MJ. Microzooplankton regulation of surface ocean POC:PON ratios. Global Biogeochem Cycles. 2016;30:311–32. doi:10.1002/2015gb005273.
11. Azam F, Smith DC, Hollibaugh JT. The role of the microbial loop in Antarctic pelagic ecosystems. Polar Res. 2016;10:239–44. doi:10.3402/polar.v10i1.6742.
12. Manganelli M, Malfatti F, Samo TJ, Mitchell BG, Wang H, Azam F. Major role of microbes in carbon fluxes during Austral winter in the Southern Drake Passage. PLoS One. 2009;4:e6941. doi:10.1371/journal.pone.0006941.
13. Fenchel T. The microbial loop-25 years later. J Exp Mar Biol Ecol. 2008;366:99–103. doi:10.1016/j.jembe.2008.07.013.
14. Romera-Castillo C, Álvarez M, Pelegrí JL, Hansell DA, Álvarez-Salgado XA. Net Additions of Recalcitrant Dissolved Organic Carbon in the Deep Atlantic Ocean. Global Biogeochem Cycles. 2019;33:1162–73. doi:10.1029/2018gb006162.
15. Ki B, Park S, Choi JH. Production of recalcitrant organic matter under the influence of elevated carbon dioxide and temperature. Water Environ Res. 2014;86:779–87. doi:10.2175/106143014x13975035526347.
16. Ogawa H, Amagai Y, Koike I, Kaiser K, Benner R. Production of refractory dissolved organic matter by bacteria. Science. 2001;292:917–20. doi:10.1126/science.1057627.
17. Koch BP, Kattner G, Witt M, Passow U. Molecular insights into the microbial formation of marine dissolved organic matter: recalcitrant or labile? Biogeosciences. 2014;11:4173–90. doi:10.5194/bg-11-4173-2014.
18. Gruber DF, Simjouw JP, Seitzinger SP, Taghon GL. Dynamics and characterization of refractory dissolved organic matter produced by a pure bacterial culture in an experimental predator-prey system. Appl Environ Microbiol. 2006;72:4184–91. doi:10.1128/AEM.02882-05.
19. Chen CT. (2011) Microbial carbon pump: additional considerations. Nat Rev Microbiol 9: 555; author reply 555. doi: 10.1038/nrmicro2386-c4.
20. Jiao N, Herndl GJ, Hansell DA, Benner R, Kattner G, Wilhelm SW, Kirchman DL, Weinbauer MG, Luo T, Chen F, Azam F. Microbial production of recalcitrant dissolved organic matter: long-term carbon storage in the global ocean. Nat Rev Microbiol. 2010;8:593–9. doi:10.1038/nrmicro2386.
21. Shen Y, Benner R. Mixing it up in the ocean carbon cycle and the removal of refractory dissolved organic carbon. Sci Rep. 2018;8:2542. doi:10.1038/s41598-018-20857-5.
22. Jiao N, Robinson C, Azam F, Thomas H, Baltar F, Dang H, Hardman-Mountford NJ, Johnson M, Kirchman DL, Koch BP, Legendre L, Li C, Liu J, Luo T, Luo YW, Mitra A, Romanou A, Tang K, Wang X, Zhang C, Zhang R. Mechanisms of microbial carbon sequestration in the ocean – future research directions. Biogeosciences. 2014;11:5285–306. doi:10.5194/bg-11-5285-2014.
23. Jiao NZ, Herndl GJ, Hansell DA, Benner R, Kattner G, Wilhelm SW, Kirchman DL, Weinbauer MG, Luo TW, Chen F, Azam F. The microbial carbon pump and the oceanic recalcitrant dissolved organic

matter pool. Nat Rev Microbiol. 2011;9:555–5. doi:10.1038/nrmicro2386-c5.

24. Legendre L, Rivkin RB, Weinbauer MG, Guidi L, Uitz J. The microbial carbon pump concept: Potential biogeochemical significance in the globally changing ocean. Prog Oceanogr. 2015;134:432–50. doi:10.1016/j.pocean.2015.01.008.
25. Zhang CL, Dang HY, Azam F, Benner R, Legendre L, Passow U, Polimene L, Robinson C, Suttle CA, Jiao NZ. Evolving paradigms in biological carbon cycling in the ocean. National Science Review. 2018;5:481–99. doi:10.1093/nsr/nwy074.
26. Kharbush JJ, Close HG, Van Mooy BAS, Arnosti C, Smittenberg RH, Le Moigne FAC, Mollenhauer G, Scholz-Bottcher B, Obreht I, Koch BP, Becker KW, Iversen MH, Mohr W. (2020) Particulate Organic Carbon Deconstructed: Molecular and Chemical Composition of Particulate Organic Carbon in the Ocean. Frontiers in Marine Science 7. doi: ARTN 518. 10.3389/fmars.2020.00518.
27. Baumas CMJ, Le Moigne FAC, Garel M, Bhairy N, Guasco S, Riou V, Armougom F, Grossart HP, Tamburini C. Mesopelagic microbial carbon production correlates with diversity across different marine particle fractions. ISME J. 2021;15:1695–708. doi:10.1038/s41396-020-00880-z.
28. Liu S, Deng Y, Jiang Z, Wu Y, Huang X, Macreadie PI. Nutrient loading diminishes the dissolved organic carbon drawdown capacity of seagrass ecosystems. Sci Total Environ. 2020;740:140185. doi:10.1016/j.scitotenv.2020.140185.
29. Duret MT, Lampitt RS, Lam P. Prokaryotic niche partitioning between suspended and sinking marine particles. Environ Microbiol Rep. 2019;11:386–400. doi:10.1111/1758-2229.12692.
30. Wang X, Zhang Y, Li Y, Luo Y-L, Pan Y-R, Liu J, Butler D. (2021) Alkaline environments benefit microbial K-strategists to efficiently utilize protein substrate and promote valorization of protein waste into short-chain fatty acids. Chem Eng J 404. doi:10.1016/j.cej.2020.127147.
31. Teeling H, Fuchs BM, Becher D, Klockow C, Gardebrecht A, Bennke CM, Kassabgy M, Huang S, Mann AJ, Waldmann J, Weber M, Klindworth A, Otto A, Lange J, Bernhardt J, Reinsch C, Hecker M, Peplies J, Bockelmann FD, Callies U, Gerdts G, Wichels A, Wiltshire KH, Glockner FO, Schweder T, Amann R. Substrate-controlled succession of marine bacterioplankton populations induced by a phytoplankton bloom. Science. 2012;336:608–11. doi:10.1126/science.1218344.
32. Dybwad C, Assmy P, Olsen LM, Peeken I, Nikolopoulos A, Krumpen T, Randelhoff A, Tatarek A, Wiktor JM, Reigstad M. (2021) Carbon Export in the Seasonal Sea Ice Zone North of Svalbard From Winter to Late Summer. Frontiers in Marine Science 7. doi: ARTN 525800. 10.3389/fmars.2020.525800.
33. Hung J-J, Tung C-H, Lin Z-Y, Chen Y-lL, Lin PS-H, Tsai Y-H L-S. Active and passive fluxes of carbon, nitrogen, and phosphorus in the northern South China Sea. Biogeosciences. 2021;18:5141–62. doi:10.5194/bg-18-5141-2021.
34. Garcia CA, Baer SE, Garcia NS, Rauschenberg S, Twining BS, Lomas MW, Martiny AC. Nutrient supply controls particulate elemental concentrations and ratios in the low latitude eastern Indian Ocean. Nat Commun. 2018;9:4868. doi:10.1038/s41467-018-06892-w.
35. Moutin T, Raimbault P. Primary production, carbon export and nutrients availability in western and eastern Mediterranean Sea in early summer 1996 (MINOS cruise). J Mar Syst. 2002;33-34:273–88.

doi:10.1016/s0924-7963(02)00062-3.

36. Hernandez-Magana AE, Liu Y, Debeljak P, Crispi O, Marie B, Koedooder C, Obernosterer I. (2021) Prokaryotic diversity and activity in contrasting productivity regimes in late summer in the Kerguelen region (Southern Ocean). Journal of Marine Systems 221. doi: ARTN 103561. 10. 1016/j.jmarsys.2021.103561.
37. Liu ST, Parsons R, Opalk K, Baetge N, Giovannoni S, Bolanos LM, Kujawinski EB, Longnecker K, Lu YH, Halewood E, Carlson CA. Different carboxyl-rich alicyclic molecules proxy compounds select distinct bacterioplankton for oxidation of dissolved organic matter in the mesopelagic Sargasso Sea. Limnol Oceanogr. 2020;65:1532–53. doi:10.1002/lno.11405.
38. Kamalanathan M, Doyle SM, Xu C, Achberger AM, Wade TL, Schwehr K, Santschi PH, Sylvan JB, Quigg A. (2020) Exoenzymes as a Signature of Microbial Response to Marine Environmental Conditions. mSystems 5. doi: 10.1128/mSystems.00290-20.
39. Manna V, De Vittor C, Giani M, Del Negro P, Celussi M. Long-term patterns and drivers of microbial organic matter utilization in the northernmost basin of the Mediterranean Sea. Mar Environ Res. 2021;164:105245. doi:10.1016/j.marenvres.2020.105245.
40. Antunes JT, Sousa AGG, Azevedo J, Rego A, Leao PN, Vasconcelos V. (2020) Distinct Temporal Succession of Bacterial Communities in Early Marine Biofilms in a Portuguese Atlantic Port. Front Microbiol 11: 1938. doi: 10.3389/fmicb.2020.01938.
41. Hwang J, Druffel ERM, Eglinton TI. (2010) Widespread influence of resuspended sediments on oceanic particulate organic carbon: Insights from radiocarbon and aluminum contents in sinking particles. Global Biogeochemical Cycles 24: n/a-n/a. doi: Artn Gb4016. 10. 1029/2010gb003802.
42. Kong LF, Yan KQ, Xie ZX, He YB, Lin L, Xu HK, Liu SQ, Wang DZ. Metaproteomics Reveals Similar Vertical Distribution of Microbial Transport Proteins in Particulate Organic Matter Throughout the Water Column in the Northwest Pacific Ocean. Front Microbiol. 2021;12:629802. doi:10.3389/fmicb.2021.629802.
43. Painter SC, Hartman SE, Kivimae C, Salt LA, Clargo NM, Daniels CJ, Bozec Y, Daniels L, Allen S, Hemsley VS, Moschonas G, Davidson K. The elemental stoichiometry (C, Si, N, P) of the Hebrides Shelf and its role in carbon export. Prog Oceanogr. 2017;159:154–77. doi:10.1016/j.pocean.2017.10.001.
44. Van Mooy BAS, Keil RG, Devol AH (2002) Impact of suboxia on sinking particulate organic carbon: Enhanced carbon flux and preferential degradation of amino acids via denitrification. Geochimica et Cosmochimica Acta 66: 457-465. doi: 10.1016/s0016-7037(01)00787-6
45. Keil RG, Neibauer JA, Biladeau C, van der Elst K, Devol AH (2016) A multiproxy approach to understanding the "enhanced" flux of organic matter through the oxygen-deficient waters of the Arabian Sea. Biogeosciences 13: 2077-2092. doi: 10.5194/bg-13-2077-2016
46. Dekas AE, Parada AE, Mayali X, Fuhrman JA, Wollard J, Weber PK, Pett-Ridge J. Characterizing Chemoautotrophy and Heterotrophy in Marine Archaea and Bacteria With Single-Cell Multi-isotope NanoSIP. Front Microbiol. 2019;10:2682. doi:10.3389/fmicb.2019.02682.

47. Devol AH, Hartnett HE. Role of the oxygen-deficient zone in transfer of organic carbon to the deep ocean. Limnol Oceanogr. 2001;46:1684–90. doi:10.4319/lo.2001.46.7.1684.
48. Bacosa HP, Kamalanathan M, Chiu MH, Tsai SM, Sun L, Labonte JM, Schwehr KA, Hala D, Santschi PH, Chin WC, Quigg A. Extracellular polymeric substances (EPS) producing and oil degrading bacteria isolated from the northern Gulf of Mexico. PLoS One. 2018;13:e0208406. doi:10.1371/journal.pone.0208406.
49. Giovannoni SJ, Cameron Thrash J, Temperton B. Implications of streamlining theory for microbial ecology. ISME J. 2014;8:1553–65. doi:10.1038/ismej.2014.60.
50. Lauro FM, McDougald D, Thomas T, Williams TJ, Egan S, Rice S, DeMaere MZ, Ting L, Ertan H, Johnson J, Ferriera S, Lapidus A, Anderson I, Kyrpides N, Munk AC, Detter C, Han CS, Brown MV, Robb FT, Kjelleberg S, Cavicchioli R. The genomic basis of trophic strategy in marine bacteria. Proc Natl Acad Sci U S A. 2009;106:15527–33. doi:10.1073/pnas.0903507106.
51. Carreira C, Talbot S, Lonborg C. Bacterial consumption of total and dissolved organic carbon in the Great Barrier Reef. Biogeochemistry. 2021;154:489–508. doi:10.1007/s10533-021-00802-x.
52. Kusch S, Wakeham SG, Dildar N, Zhu C, Sepulveda J. Bacterial and archaeal lipids trace chemo(auto)trophy along the redoxcline in Vancouver Island fjords. Geobiology. 2021;19:521–41. doi:10.1111/gbi.12446.
53. Landa M, Cottrell MT, Kirchman DL, Kaiser K, Medeiros PM, Tremblay L, Batailler N, Caparros J, Catala P, Escoubeyrou K, Oriol L, Blain S, Obernosterer I. Phylogenetic and structural response of heterotrophic bacteria to dissolved organic matter of different chemical composition in a continuous culture study. Environ Microbiol. 2014;16:1668–81. doi:10.1111/1462-2920.12242.
54. D'Andrilli J, Junker JR, Smith HJ, Scholl EA, Foreman CM. DOM composition alters ecosystem function during microbial processing of isolated sources. Biogeochemistry. 2019;142:281–98. doi:10.1007/s10533-018-00534-5.
55. Zhao Z, Gonsior M, Schmitt-Kopplin P, Zhan Y, Zhang R, Jiao N, Chen F. Microbial transformation of virus-induced dissolved organic matter from picocyanobacteria: coupling of bacterial diversity and DOM chemodiversity. ISME J. 2019;13:2551–65. doi:10.1038/s41396-019-0449-1.
56. Beier S, Bertilsson S. Bacterial chitin degradation-mechanisms and ecophysiological strategies. Front Microbiol. 2013;4:149. doi:10.3389/fmicb.2013.00149.
57. Li JT, Gu LY, Bai SJ, Wang J, Su L, Wei BB, Zhang L, Fang JS. Characterization of particle-associated and free-living bacterial and archaeal communities along the water columns of the South China Sea. Biogeosciences. 2021;18:113–33. doi:10.5194/bg-18-113-2021.
58. Wells LE, Cordray M, Bowerman S, Miller LA, Vincent WF, Deming JW. Archaea in particle-rich waters of the Beaufort Shelf and Franklin Bay, Canadian Arctic: Clues to an allochthonous origin? Limnol Oceanogr. 2006;51:47–59. doi:10.4319/lo.2006.51.1.0047.
59. Lam P, Kuypers MM. Microbial nitrogen cycling processes in oxygen minimum zones. Ann Rev Mar Sci. 2011;3:317–45. doi:10.1146/annurev-marine-120709-142814.

60. Kim JG, Gazi KS, Awala SI, Jung MY, Rhee SK. Ammonia-oxidizing archaea in biological interactions. J Microbiol. 2021;59:298–310. doi:10.1007/s12275-021-1005-z.
61. Momper LM, Reese BK, Carvalho G, Lee P, Webb EA. A novel cohabitation between two diazotrophic cyanobacteria in the oligotrophic ocean. ISME J. 2015;9:882–93. doi:10.1038/ismej.2014.186.
62. Wang Y, Liao S, Gai Y, Liu G, Jin T, Liu H, Gram L, Strube ML, Fan G, Sahu SK, Liu S, Gan S, Xie Z, Kong L, Zhang P, Liu X, Wang DZ. Metagenomic Analysis Reveals Microbial Community Structure and Metabolic Potential for Nitrogen Acquisition in the Oligotrophic Surface Water of the Indian Ocean. Front Microbiol. 2021;12:518865. doi:10.3389/fmicb.2021.518865.
63. Moisander PH, Benavides M, Bonnet S, Berman-Frank I, White AE, Riemann L. Chasing after Non-cyanobacterial Nitrogen Fixation in Marine Pelagic Environments. Front Microbiol. 2017;8:1736. doi:10.3389/fmicb.2017.01736.
64. Polerecky L, Masuda T, Eichner M, Rabouille S, Vancova M, Kienhuis MVM, Bernat G, Bonomi-Barufi J, Campbell DA, Claquin P, Cerveny J, Giordano M, Kotabova E, Kromkamp J, Lombardi AT, Lukes M, Prasil O, Stephan S, Suggett D, Zavrel T, Halsey KH. Temporal Patterns and Intra- and Inter-Cellular Variability in Carbon and Nitrogen Assimilation by the Unicellular Cyanobacterium Cyanothece sp. ATCC 51142. Front Microbiol. 2021;12:620915. doi:10.3389/fmicb.2021.620915.
65. Mettam C, Zerkle AL, Claire MW, Prave AR, Poulton SW, Junium CK. (2019) Anaerobic nitrogen cycling on a Neoarchaean ocean margin. Earth and Planetary Science Letters 527. doi: ARTN 115800. 10.1016/j.epsl.2019.115800.
66. Trull TW, Bray SG, Manganini SJ, Honjo S, Francois R. Moored sediment trap measurements of carbon export in the Subantarctic and Polar Frontal Zones of the Southern Ocean, south of Australia. Journal of Geophysical Research-Oceans. 2001;106:31489–509. Doi 10.1029/2000jc000308. doi.
67. de Boyer Montégut C. (2004) Mixed layer depth over the global ocean: An examination of profile data and a profile-based climatology. J Geophys Res 109. doi:10.1029/2004jc002378.
68. Riley JS, Sanders R, Marsay C, Le Moigne FAC, Achterberg EP, Poulton AJ. (2012) The relative contribution of fast and slow sinking particles to ocean carbon export. Global Biogeochem Cycles 26: n/a-n/a. doi:10.1029/2011gb004085.
69. Fontanez KM, Eppley JM, Samo TJ, Karl DM, DeLong EF. Microbial community structure and function on sinking particles in the North Pacific Subtropical Gyre. Front Microbiol. 2015;6:469. doi:10.3389/fmicb.2015.00469.
70. Silva GG, Green KT, Dutilh BE, Edwards RA. SUPER-FOCUS: a tool for agile functional analysis of shotgun metagenomic data. Bioinformatics. 2016;32:354–61. doi:10.1093/bioinformatics/btv584.
71. Hirai M, Nishi S, Tsuda M, Sunamura M, Takaki Y, Nunoura T. Library Construction from Subnanogram DNA for Pelagic Sea Water and Deep-Sea Sediments. Microbes Environ. 2017;32:336–43. doi:10.1264/jsme2.ME17132.
72. Bolger AM, Lohse M, Usadel B. Trimmomatic: a flexible trimmer for Illumina sequence data. Bioinformatics. 2014;30:2114–20. doi:10.1093/bioinformatics/btu170.

73. Kieser S, Brown J, Zdobnov EM, Trajkovski M, McCue LA. ATLAS: a Snakemake workflow for assembly, annotation, and genomic binning of metagenome sequence data. BMC Bioinformatics. 2020;21:257. doi:10.1186/s12859-020-03585-4.
74. Parks DH, Imelfort M, Skennerton CT, Hugenholtz P, Tyson GW. CheckM: assessing the quality of microbial genomes recovered from isolates, single cells, and metagenomes. Genome Res. 2015;25:1043–55. doi:10.1101/gr.186072.114.
75. Bowers RM, Kyrpides NC, Stepanauskas R, Harmon-Smith M, Doud D, Reddy TBK, Schulz F, Jarett J, Rivers AR, Eloe-Fadrosh EA, Tringe SG, Ivanova NN, Copeland A, Clum A, Becraft ED, Malmstrom RR, Birren B, Podar M, Bork P, Weinstock GM, Garrity GM, Dodsworth JA, Yooseph S, Sutton G, Glockner FO, Gilbert JA, Nelson WC, Hallam SJ, Jungbluth SP, Ettema TJG, Tighe S, Konstantinidis KT, Liu WT, Baker BJ, Rattei T, Eisen JA, Hedlund B, McMahon KD, Fierer N, Knight R, Finn R, Cochrane G, Karsch-Mizrachi I, Tyson GW, Rinke C, Genome Standards C, Lapidus A, Meyer F, Yilmaz P, Parks DH, Eren AM, Schriml L, Banfield JF, Hugenholtz P, Woyke T. Minimum information about a single amplified genome (MISAG) and a metagenome-assembled genome (MIMAG) of bacteria and archaea. Nat Biotechnol. 2017;35:725–31. doi:10.1038/nbt.3893.
76. Chaumeil PA, Mussig AJ, Hugenholtz P, Parks DH. GTDB-Tk: a toolkit to classify genomes with the Genome Taxonomy Database. Bioinformatics. 2019. doi:10.1093/bioinformatics/btz848.
77. Jain C, Rodriguez RL, Phillippy AM, Konstantinidis KT, Aluru S. High throughput ANI analysis of 90K prokaryotic genomes reveals clear species boundaries. Nat Commun. 2018;9:5114. doi:10.1038/s41467-018-07641-9.
78. Shaffer M, Borton MA, McGivern BB, Zayed AA, La Rosa SL, Solden LM, Liu P, Narrowe AB, Rodriguez-Ramos J, Bolduc B, Gazitua MC, Daly RA, Smith GJ, Vik DR, Pope PB, Sullivan MB, Roux S, Wrighton KC. DRAM for distilling microbial metabolism to automate the curation of microbiome function. Nucleic Acids Res. 2020;48:8883–900. doi:10.1093/nar/gkaa621.

Figures

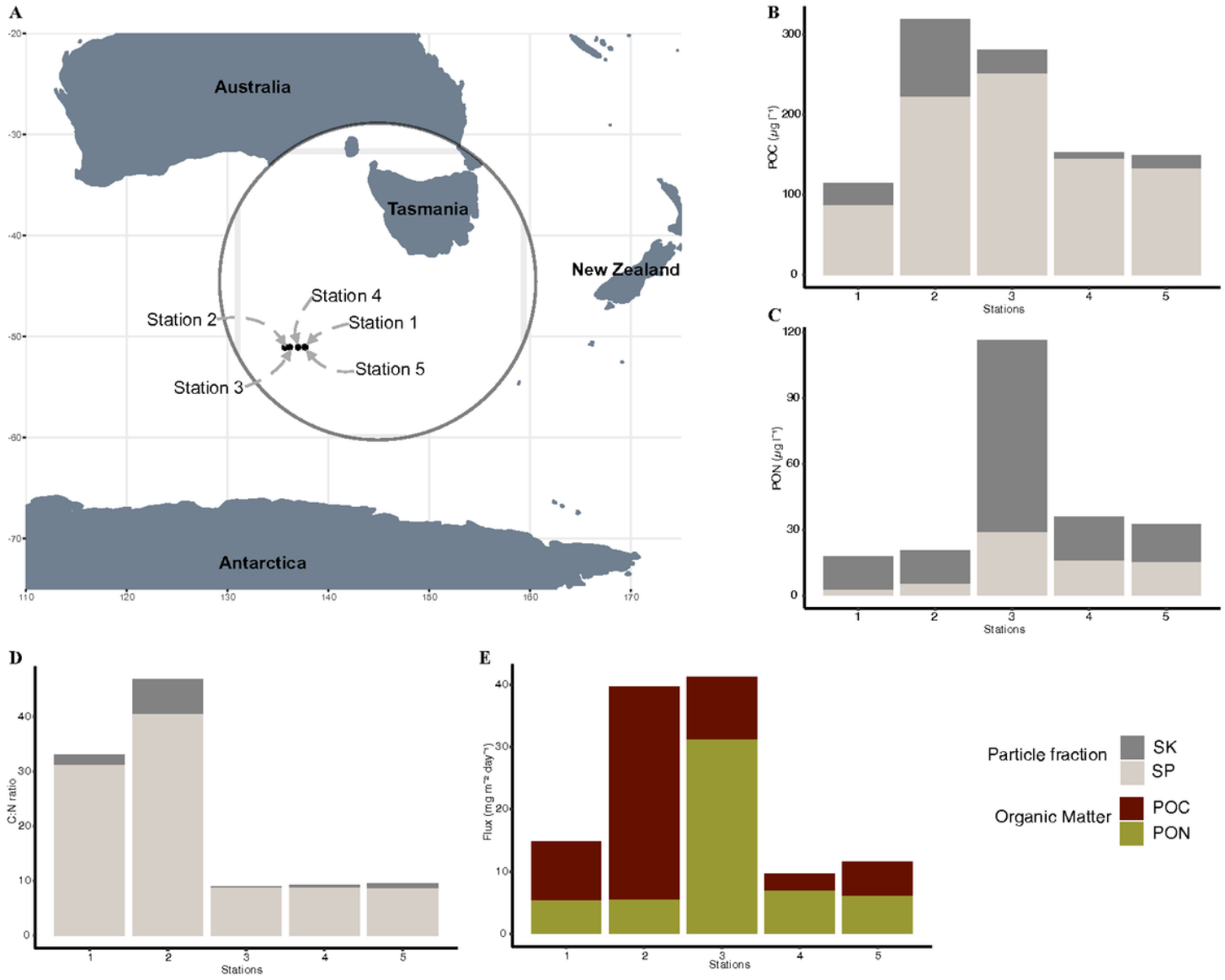

Figure 1

Marine Snow Catcher (MSC) deployment at SOTS site during the IN2019_V02 using RV investigator collecting POC and PON from suspended (SP) and sinking (SK) particle-pool. A) The sampling location at the SOTS site, B) POC concentration for SP (green bar) and SK (blue bar), C) PON concentration for SP and SK, D) POC:PON ratio for SP and SK and E) POC and PON export flux at five stations.

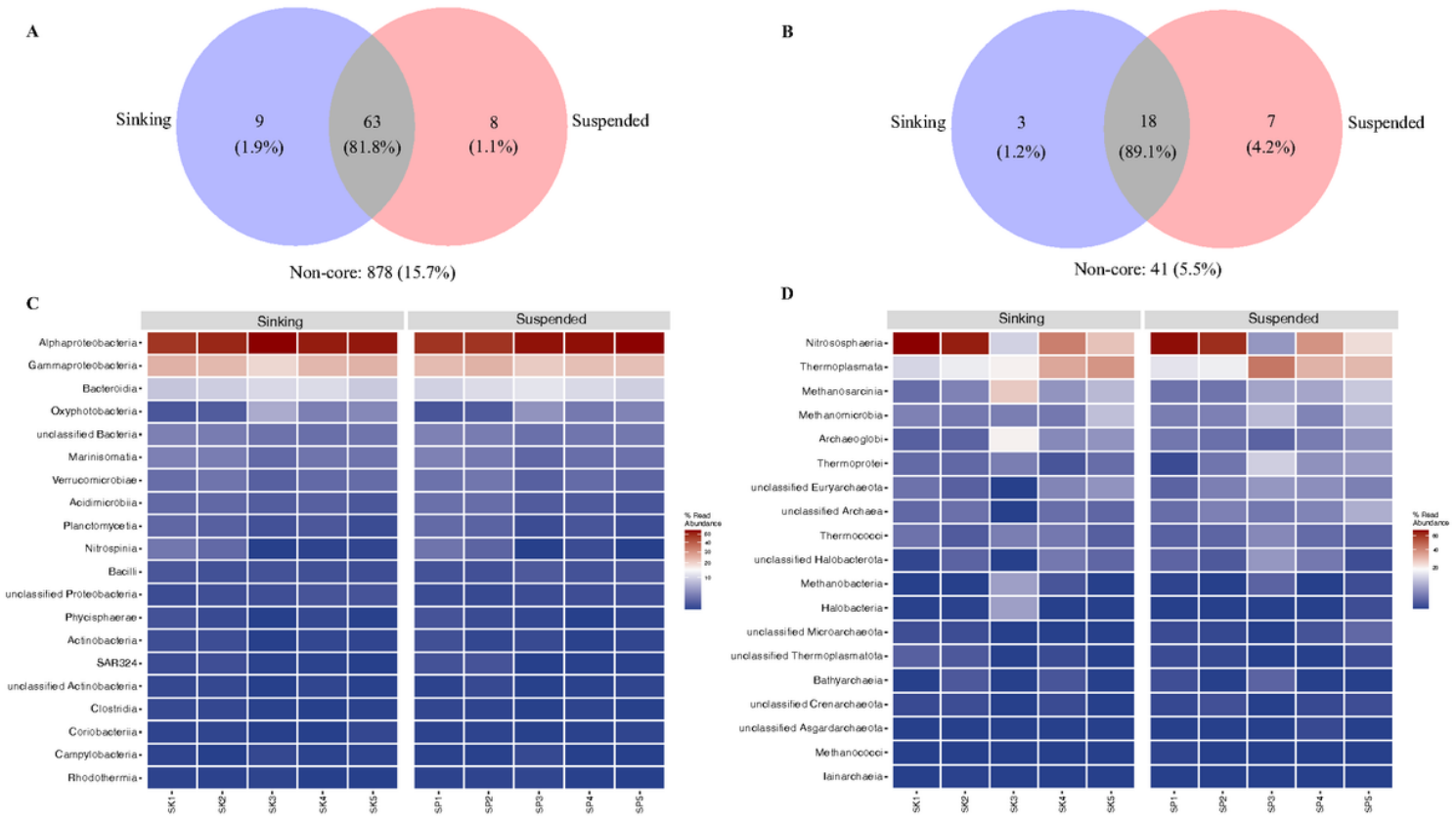

Figure 2

Taxonomic composition and distribution of the SOTS prokaryotic community determined by single copy marker genes (ribosomal protein genes) using SingleM pipeline. A) Venn diagram showing the core OTU shared by suspended and sinking bacterial taxonomic composition. B) Heatmap showing the percentage read abundances (%) of the bacterial class composition in the suspended and sinking at each station, taxa with low abundance are coloured blue, those in higher abundance are white, while the highest are in red. C) Venn diagram showing the core OTU percentage read abundance shared by suspended and sinking archaeal taxonomic composition. D) Heatmap showing the percentage read abundances (%) of the archaeal class in the suspended and sinking at each station.

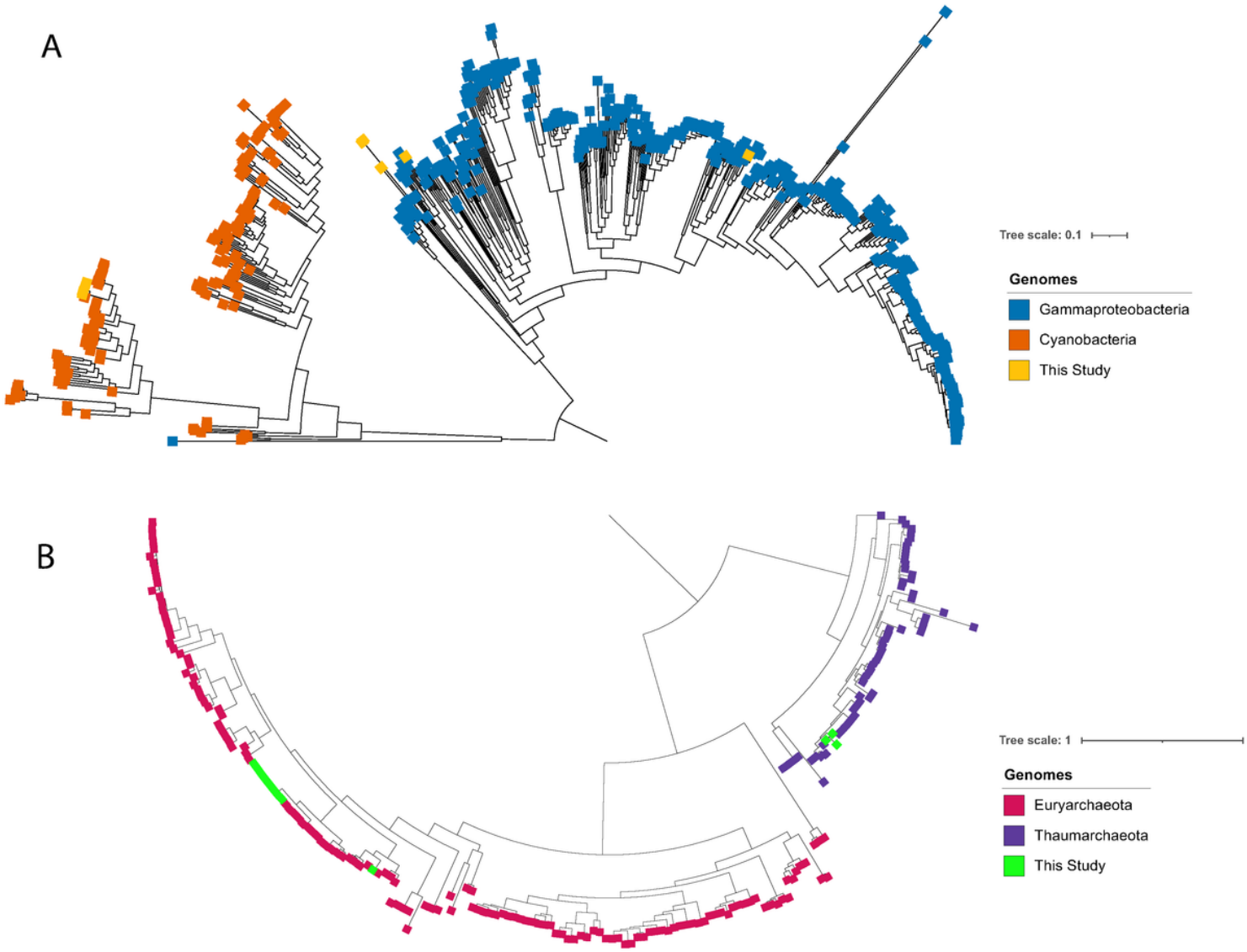

Figure 3

Phylogenomic inference of our 24 MAGs. The phylogenomic tree was based on alignment of 40% of the marker gene present in our MAGs. A) Bacterial MAGs (yellow) against Gammaproteobacteria (blue) and Cyanobacteria (orange). B) Archaeal MAGs (green) against Euryarchaeota (red) and Thaumarchaeota (purple).

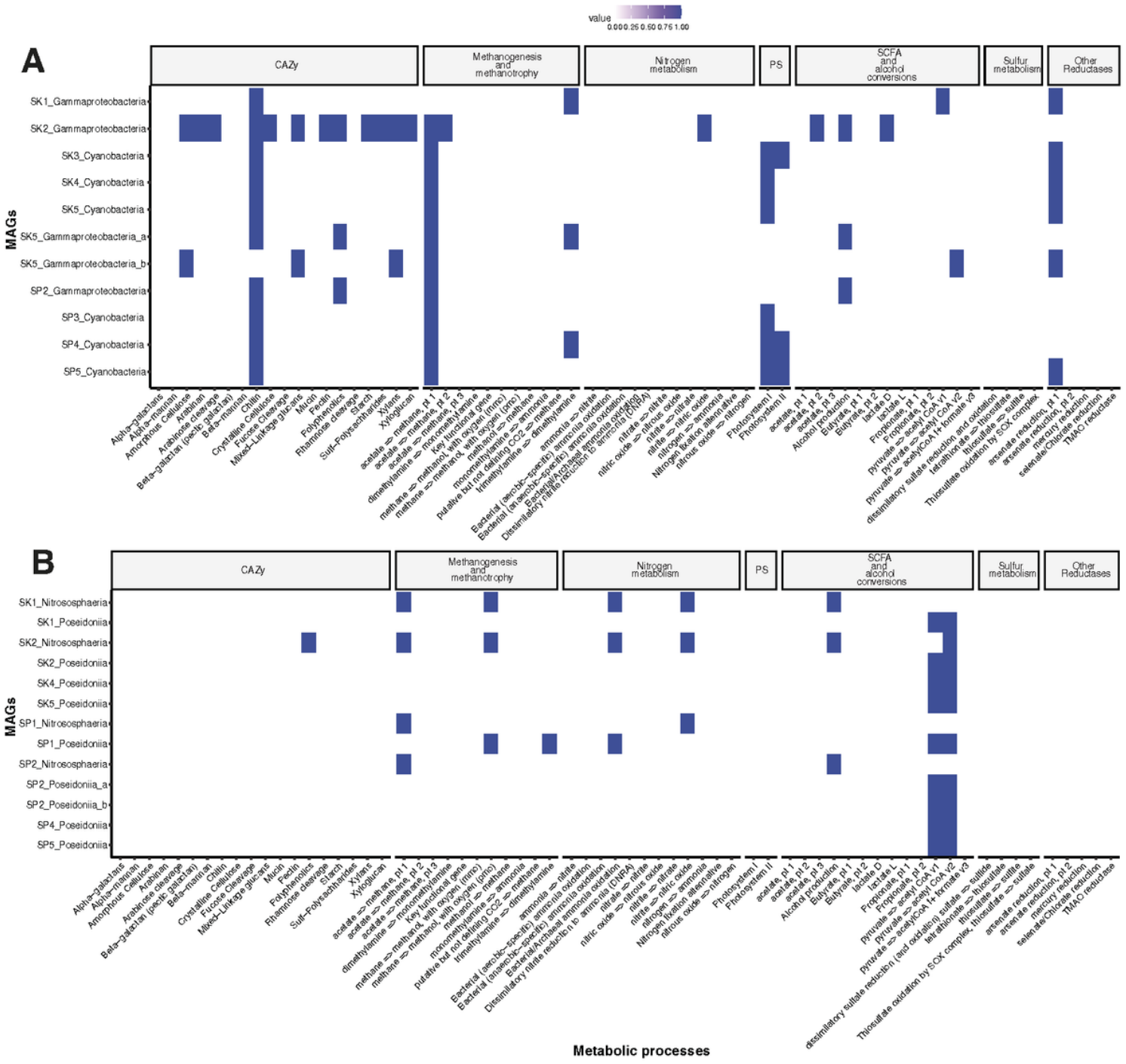

Figure 4

The presence of potential complex metabolism of 24 MAGs for carbohydrates metabolism, nitrogen metabolism, etc. based on DRAM pipeline. A) Bacterial functional annotation and B) Archaeal functional annotation.

Supplementary Files

This is a list of supplementary files associated with this preprint. Click to download.

- FigureS1.pdf
- FigureS2.pdf
- FigureS3.pdf
- FigureS4.pdf
- SupplementaryMaterialsforDithugoeetal.docx
- SupplementaryTables.xlsx